Enhancement of endotoxin neutralization by coupling of a C12-alkyl chain to a lactoferricin-derived peptide

Jörg ANDRÄ*[1], Karl LOHNER†, Sylvie E. BLONDELLE‡, Roman JERALA§, Ignacio MORIYON‖, Michel H. J. KOCH¶, Patrick GARIDEL** and Klaus BRANDENBURG*

*Research Center Borstel, Leibniz-Center for Medicine and Biosciences, Division of Biophysics, Parkallee 10, D-23845 Borstel, Germany, †Österreichische Akademie der Wissenschaften, Institut für Biophysik und Röntgenstrukturforschung, Schmiedlstrasse 6, A-8042 Graz, Austria, ‡Torrey Pines Institute for Molecular Studies, Department of Biochemistry/Microbiology, 3550 General Atomics Court, San Diego, CA 92121, U.S.A., §National Institute of Chemistry, Hajdrihova 19, 1000 SL-Ljubljana, Slovenia, ‖Universidad de Navarra, Departamento de Microbiologia, Irunlarrea 1, 31008 Pamplona, Spain, ¶European Molecular Biology Laboratory, EMBL c/o DESY, Hamburg outstation, Notkestrasse 85, D-22603 Hamburg, Germany, and **Martin-Luther-Universität Halle/Wittenberg, Institut für Physikalische Chemie, Mühlpforte 1, D-06108 Halle/Saale, Germany

Antibacterial peptide acylation, which mimics the structure of the natural lipopeptide polymyxin B, increases antimicrobial and endotoxin-neutralizing activities. The interaction of the lactoferricin-derived peptide LF11 and its N-terminally acylated analogue, lauryl-LF11, with different chemotypes of bacterial lipopolysaccharide (LPS Re, Ra and smooth S form) was investigated by biophysical means and was related to the peptides' biological activities. Both peptides exhibit high antibacterial activity against the three strains of *Salmonella enterica* differing in the LPS chemotype. Lauryl-LF11 has one order of magnitude higher activity against Re-type, but activity against Ra- and S-type bacteria is comparable with that of LF11. The alkyl derivative peptide lauryl-LF11 shows a much stronger inhibition of the LPS-induced cytokine induction in human mononuclear cells than LF11. Although peptide–LPS interaction is essentially of electrostatic nature, the lauryl-modified peptide displays a strong hydrophobic component. Such a feature might then explain the fact that saturation of the peptide binding takes place at a much lower peptide/LPS ratio for LF11 than for lauryl-LF11, and that an overcompensation of the negative LPS backbone charges is observed for lauryl-LF11. The influence of LF11 on the gel-to-liquid-crystalline phase-transition of LPS is negligible for LPS Re, but clearly fluidizing for LPS Ra. In contrast, lauryl-LF11 causes a cholesterol-like effect in the two chemotypes, fluidizing in the gel and rigidifying of the hydrocarbon chains in the liquid-crystalline phase. Both peptides convert the mixed unilamellar/non-lamellar aggregate structure of lipid A, the 'endotoxic principle' of LPS, into a multilamellar one. These data contribute to the understanding of the mechanisms of the peptide-mediated neutralization of endotoxin and effect of lipid modification of peptides.

Key words: antimicrobial peptide, antisepsis, endotoxin, hydrophobic extension, lactoferricin, lipopolysaccharide (LPS).

INTRODUCTION

Despite the existence of broad-range antibiotics, septic shock resulting from bacterial infection remains a frequent cause of death, particularly in intensive care units. One main therapeutic approach to combat infectious diseases is the use of the naturally occurring protein lactoferrin (LF) and its N-terminal fragment released *in vivo* after cleavage by pepsin, termed lactoferricin [1]. LF is an iron-binding protein, a major component of secondary granules of neutrophils, which is released from these cells during inflammation [2]. Lactoferricin consists of the region between amino acid residues 17 and 41 for bovine, and 1 and 45 for human, LF [3], and inhibits the growth of a broad range of bacteria and other pathogens. Its mode of action is assumed to consist in membrane perturbation [4].

In the case of Gram-negative bacteria, LPS (lipopolysaccharide; endotoxin) from the outer leaflet of the outer membrane is the first target of all antibiotics. LPS consists of a lipid part, termed lipid A, anchoring the molecule into the membrane, and a covalently linked oligo- or poly-saccharide directed outwards [5]. Lipid A is the minimal biological active unit of LPS and is thus called the 'endotoxic principle' of LPS. Since LPS is essential for the survival of Gram-negative bacteria, its release due to antibiotic attack leads to bacterial death. However, isolated endotoxin essentially contributes to the inflammation process by interacting with cellular membranes of immune cells, such as mononuclear cells, leading to the secretion of cytokines such as interleukins and TNFα (tumour necrosis factor α). Depending on the location and the amounts of LPS liberated, the outcome may be either less severe or leading to the septic shock syndrome, often with fatal consequences [6]. Thus, besides eradication of bacteria, an effective neutralization of isolated LPS is of utmost importance in the field of sepsis research. The N-terminal part of lactoferricin is effective in neutralizing LPS with a similar effectiveness as polymyxin B [7], and, in particular, a stretch of 11 amino acid residues within lactoferricin (residues 21–31) exhibited antibacterial and endotoxin-neutralizing activities [4,8]. C-terminal linkage of acyl chains to this peptide significantly enhanced the LPS-binding capacity. Most effective was the 12-carbon-unit acyl derivative [8]. We selected this sequence, now termed LF11, as a basis for the development of endotoxin-neutralizing and antibacterial drugs. In the present paper, we report the results of biophysical and biochemical investigations into the interaction between LF11 and its N-terminally linked

Abbreviations used: CMC, critical micelle concentration; DSC, differential scanning calorimetry; FTIR, Fourier transform IR; ΔH_c, phase-transition enthalpy; ITC, isothermal titration calorimetry; LB, Luria–Bertani; LBP, LPS-binding protein; LF, lactoferrin; LPS, lipopolysaccharide; MIC, minimal inhibitory concentration; MM, molecular mass; MNC, mononuclear cell; MTT, 3-(4,5-dimethylthiazol-2-yl)-2,5-diphenyl-2*H*-tetrazolium bromide; PMS, phenazine methosulphate; RBC, red blood cell; $T_{1/2}$, half-width temperature; T_c, phase-transition temperature; TNFα, tumour necrosis factor α.

[1] To whom correspondence should be addressed (email jandrae@fz-borstel.de).

12-carbon-units acyl derivative (lauryl-LF11) and LPS of varying sugar length. This comprises the characterization of the endotoxin binding to the peptide, as well as the activities in biological tests.

MATERIALS AND METHODS

Bacterial strains

Bacterial strains used were wild-type or LPS-mutant strains of *Salmonella enterica* (serovar Minnesota) with smooth-form LPS (S-form, wild-type), strain R60 (LPS Ra), and strain R595 (LPS Re). Bacteria were grown overnight in LB (Luria–Bertani) medium, composed of 1 % tryptone, 0.5 % yeast extract and 1 % NaCl, under constant shaking at 37 °C, and subsequently inoculated in the same medium to reach the mid-exponential phase.

Lipids

Bacteria grown at 37 °C were phenol-extracted, treated with RNase, DNase and proteinase, dialysed, and freeze-dried. From this freeze-dried sample, LPS from rough mutants Re (strain R595) and Ra (strain R60) from *S. enterica* were extracted by the phenol/chloroform/light petroleum method [9], purified, and freeze-dried. Smooth-form LPS from *S. enterica* was extracted according to the phenol/water procedure [10]. Free lipid A was isolated by acetate buffer treatment of LPS R595. After isolation, the resulting lipid A was purified and converted into its triethylamine salt.

Peptides

The peptides LF11 [FQWQRNIRKVR-NH_2, MM (molecular mass) = 1529.8 Da] and lauryl-LF11 [CH_3-$(CH_2)_{10}$-CO-NH-FQWQRNIRKVR-NH_2, MM = 1712.1 Da] were purchased from NeoMPS (San Diego, CA, U.S.A.). The purities were > 96 % as determined by RP (reverse-phase)-HPLC and MS. Melittin (HPLC grade, MM = 2846.5 Da) was purchased as synthetic peptide from Sigma (Deisenhofen, Germany) and used without further purification.

Preparation of endotoxin aggregates

LPS or lipid A was solubilized in the respective buffer (lipid concentration 1–10 mM, depending on the applied technique), extensively vortex-mixed, sonicated for 30 min, and subjected to several temperature cycles between 20 and 60 °C. Finally, the lipid suspension was incubated at 4 °C for at least 12 h before use.

Assay for antibacterial activity

Peptides were dissolved at a concentration of 100 μg/ml (LF11 and lauryl-LF11) or up to 25 μg/ml (melittin) in 20 mM Hepes, pH 7.0, and 180 μl of this solution filled the first well of a microtitre plate. For a 2-fold serial dilution, each 90 μl was transferred to the next well filled with the same volume of buffer. Subsequently, a suspension of exponential-phase bacteria in LB was added (10 μl, containing 10^4 colony forming units) to the peptide solution (90 μl). The plates were incubated overnight in a wet chamber at 37 °C under constant shaking, and bacterial growth was monitored by measuring the attenuance at 620 nm in a microtitre-plate reader (Rainbow, Tecan, Crailsham, Germany). The MIC (minimal inhibitory concentration) was defined as the lowest peptide concentration, where no bacterial growth was measurable. Portions of each well (10 μl) were diluted with 90 μl of Hepes buffer, plated out in duplicate on LB-agar plates, incubated overnight at 37 °C, and bacterial colonies were counted. The MBC (minimal bactericidal concentration) was defined as the peptide concentration where no colony growth was observed. Experiments were performed at least twice in duplicates.

Stimulation of human MNCs (mononuclear cells) by LPS

MNCs were isolated from heparinized blood of healthy donors as described previously [11]. The cells were resuspended in medium (RPMI 1640) and their number was equilibrated at 5×10^6 cells/ml. For stimulation, 200 μl of MNC suspension (1×10^6 cells) was transferred into each well of a 96-well culture plate. LPS and peptide/LPS mixtures were incubated for 30 min at 37 °C, and added to the cultures at 20 μl per well. The cultures were incubated for 4 h at 37 °C under 5 % CO_2. Supernatants were collected after centrifugation of the culture plates for 10 min at 400 ***g*** and stored at − 20 °C until determination of TNFα content. Immunological determination of TNFα was carried out in a sandwich ELISA using a monoclonal antibody against TNF (clone 6b from Intex AG, Muttenz, Switzerland) and has been described in detail previously [11].

Assay for haemolytic activity

RBCs (red blood cells) were obtained from citrated human blood by centrifugation (1500 ***g***, 10 min), washed three times with isotonic 20 mM phosphate/NaCl buffer (pH 7.4), and suspended in the same buffer at a concentration equivalent to 5 % of the normal haematocrit. Aliquots of 40 μl of this RBC suspension were added to 0.96 ml of peptide dilutions prepared in the same isotonic phosphate solution, incubated at 37 °C for 30 min and centrifuged (1500 ***g***, 10 min). The supernatants were analysed spectrophotometrically (absorbance at 543 nm) for haemoglobin, and results are expressed as the percentage released with respect to sonicated controls (100 % release) or controls processed without peptides (0 % release) [12].

Cytotoxicity assay

Cytotoxicity was assayed on HeLa cells by two independent methods, the MTT [3-(4,5-dimethylthiazol-2-yl)-2,5-diphenyl-2*H*-tetrazolium bromide]-PMS (phenazine methosulphate) assay, which assesses the performance of the respiratory chain by the reduction of a tetrazolium base compound to a blue formazan product [13], and the Trypan Blue exclusion test, which assesses alterations in membrane integrity as determined by the uptake of this dye by dead cells [14]. In both protocols, cells were grown in DMEM (Dulbecco's modified Eagle's medium) (Invitrogen S.A., Barcelona, Spain) to a density of 5×10^5 cells/ml and distributed (100 μl or 50 000 cells/well) in 96-well (flat-bottom) polystyrene plates. Plates were incubated for 16 h at 37 °C in a 5 % CO_2 atmosphere, then supplemented with increasing amounts of peptides diluted in 20 mM Hepes, pH 7.2, and incubation was carried on for 20 h under the same conditions. Preliminary experiments showed that these conditions increased the sensitivity of the methods, while keeping spontaneous cell decay at background levels. After this time, 0.22-μm-filtered MTT (Promega Biosciences, San Luis Obispo, CA, U.S.A.) and PMS (Sigma Chemical Co., St. Louis, MO, U.S.A.) solutions (at 2 and 0.92 mg/ml respectively) in Dulbecco's PBS (2.68 mM KCl, 137 mM NaCl, 1.47 mM KH_2PO_4, 8.1 mM Na_2HPO_4, 0.9 mM $CaCl_2$ and 0.5 mM $MgCl_2$, pH 6.5) were mixed in a 20:1 proportion in the dark, and 25 μl of the mixture was added to each well. After 30 min of incubation at 37 °C in a 5 % CO_2 atmosphere, the contents of the wells were mixed with gentle rotation with 100 μl of 40 mM HCl in propan-2-ol to solubilize any blue formazan crystals, and this product was measured

photometrically at 550 nm in a Tittertek Multiscan (Flow Laboratories, McLean, VA, U.S.A.) plate reader. Alternatively, an aliquot of the cells was taken (before MTT-PMS addition), mixed with an equal volume of 0.4 % (w/v) Trypan Blue (Sigma), dispensed into the chamber of a Neubauer haemocytometer, and at least 100 cells were examined for dye uptake under a phase-contrast microscope [14]. In both methods, controls were cells incubated without peptide (0 % cytotoxicity reference values) or with 10 μl of DMSO (100 % cell death reference values).

FTIR (Fourier transform IR) spectroscopy

The IR spectroscopic measurements were performed on an IFS-55 spectrometer (Bruker, Karlsruhe, Germany). Samples, dissolved in 20 mM Hepes, pH 7.0, were placed in a CaF_2 cuvette with a 12.5 μm Teflon spacer. Measurements were performed at the intrinsic instrument temperature (26 °C), or, if indicated, temperature-scans were performed automatically between 10 and 70 °C with a heating rate of 0.6 °C/min. Every 3 °C, 50 interferograms were accumulated, apodized, Fourier-transformed and converted into absorbance spectra. For strong absorption bands, the band parameters (peak position, band width and intensity) were evaluated from the original spectra, if necessary after subtraction of the strong water bands.

DSC (differential scanning calorimetry)

Endotoxin dispersions (1 mg/ml) were prepared as described above by dissolving a known amount of LPS in 10 mM phosphate buffer, pH 6.8, and the sample was degassed for 10 min. Different amounts of peptides were mixed with the endotoxin dispersion and investigated by DSC using the VP DSC unit from MicroCal Inc. (Northampton, MA, U.S.A.). The sample cell was filled with the endotoxin preparation, whereas the reference cell was filled with buffer. Heating and cooling curves were measured in the temperature interval 10–90 °C. Three consecutive heating and cooling scans were performed at a scanning rate of 1 °C/min [15]. The phase-transition enthalpy was calculated as the integral intensity of the heat capacity curve. The data were analysed using the appropriate Origin software as described previously [15].

^{45}Ca displacement

To investigate the ability of the peptides to displace divalent Ca^{2+} cations from LPS monolayers, a subphase with 12.5 μM Ca^{2+} doped with radioactive $^{45}Ca^{2+}$ (at a final activity of 250 Bq/ml; Amersham-Buchler, Braunschweig, Germany) and 5 mM Hepes, pH 7.0, were used. The experiments were performed as described in [16] using an LPS R595 monolayer (10 nmol/112 cm^2). The peptides were added to the subphase (60 ml) in different concentrations, and the equilibrium β-counting rates were recorded. The relative ^{45}Ca concentration was calculated from the equation $I_{rel} = (I_{pep} - I_{sub})/(I_{mono} - I_{sub})$, with I_{rel} = relative ^{45}Ca intensity, I_{sub}, I_{mono} and I_{pep}, the β-intensities of the pure subphase, after spreading of the monolayer and after peptide addition respectively.

Zeta potential

Zeta potentials were determined with a Zeta-Sizer 4 (Malvern Instruments, Herrsching, Germany) at a scattering angle of 90° from the electrophoretic mobility by laser-Doppler anemometry as described previously [11]. The zeta potential was calculated according to the Helmholtz–Smoluchovski equation from the mobility of the aggregates in a driving electric field of 19.2 V $\cdot$ cm^{-1}. Endotoxin aggregates (0.1 mM) and peptide stock solutions (0.5 mM) were prepared in 10 mM Tris/HCl and 2 mM CsCl, pH 7.0, which was found to give the most reproducible results.

X-ray diffraction

X-ray diffraction measurements were performed at the European Molecular Biology Laboratory (EMBL) outstation at the Hamburg synchrotron radiation facility HASYLAB using the double-focusing monochromator-mirror camera X33 [17]. Diffraction patterns in the range of the scattering vector $0.07 < s < 1$ nm^{-1} ($s = 2 \sin \theta/\lambda$; 2θ, scattering angle and λ, the wavelength = 0.15 nm) were recorded at various temperatures with exposure times of 2 or 3 min using a linear detector with delay line readout [18]. The s-axis was calibrated with tripalmitin which has a periodicity of 4.06 nm at room temperature (22 °C). Details of the data acquisition and evaluation system can be found elsewhere [19]. The diffraction patterns were evaluated as described previously [11], assigning the spacing ratios of the main scattering maxima to defined three-dimensional structures. The lamellar and cubic structures are most relevant here. They are characterized by the following features: (i) lamellar: the reflections are grouped in equidistant ratios, i.e. 1, 1/2, 1/3, 1/4 etc., of the lamellar repeat distance d_l; (ii) cubic: the different space groups of these non-lamellar three-dimensional structures differ in the ratio of their spacings. The relation between reciprocal spacing $s_{hkl} = 1/d_{hkl}$ and lattice constant a is $s_{hkl} = [(h^2 + k^2 + l^2)/a\,]_{1/2}$, where h, k and l are the Miller indices of the corresponding set of plane.

RESULTS

Antibacterial, cytotoxic and haemolytic activities of peptides

In a first step, the antibacterial activity of the two peptides LF11 and lauryl-LF11 against bacteria with LPS of different sugar-chain lengths were determined, with the well characterized peptide melittin from bee venom as a reference (Figure 1). All peptides have the highest activity against *S. enterica* (strain R595) whose outer membrane outer leaflet consists of deep rough mutant LPS Re. In particular, lauryl-LF11 and melittin exhibited comparable activity, which was considerably higher than for LF11. For bacteria with a LPS chemotype of much longer sugar chains (Ra and S-form), corresponding to a higher hydrophilicity of their LPS, the antibacterial activities of the peptides are significantly lower than for bacteria expressing LPS Re, and the activities of LF11 and its acylated derivative were the same. In contrast with their antibacterial activity, both peptides are non-cytotoxic to HeLa cells at concentrations up to 500 μg/ml. However, the acylated peptide, but not LF11, showed haemolytic activity comparable with that of melittin at concentrations above the MICs (results not shown).

Inhibition of LPS-induced cell activation by peptides

The inhibition of the LPS-induced induction of TNFα in human MNCs due to peptide binding is shown in Figure 2. For all LPS, lauryl-LF11 inhibits the cytokine induction at a concentration between 20 and 60 nM, whereas LF11 inhibits only LPS Re effectively, but at a 3-fold higher dose than lauryl-LF11.

Ca-displacement from LPS monolayers

The outer membrane of LPS of Gram-negative bacteria is stabilized by divalent cations. Disruption of the bacterial membrane integrity can be accomplished either by removal of those ions by complexation or by their replacement with polycations such as cationic peptides. The ability of the peptides to displace ^{45}Ca

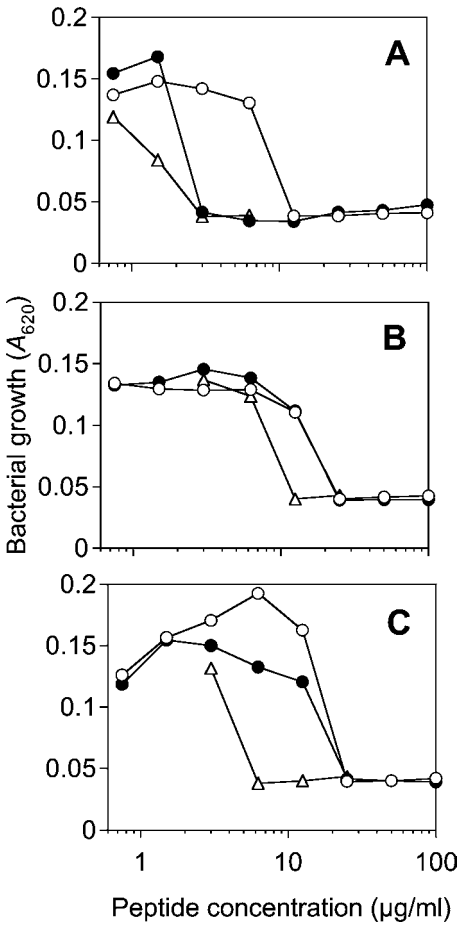

Figure 1 Antibacterial activity of lactoferricin-derived peptides LF11 (○) and lauryl-LF11 (●), compared to synthetic bee venom melittin (△) against *S. enterica* serovar Minnesota strains with variation in the LPS carbohydrate structures

(**A**) Strain R595 (LPS Re); (**B**) strain R60 (LPS Ra); (**C**) wild-type (S-form LPS).

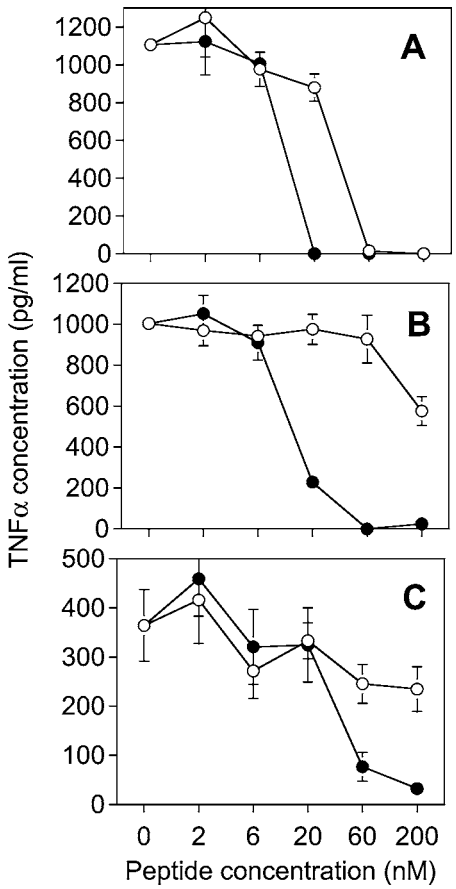

Figure 2 Concentration-dependent inhibition of the biological activity of various LPS by synthetic peptides

LF11 (○) and lauryl-LF11 (●) were incubated with 0.5 ng/ml LPS Re (**A**), 0.5 ng/ml LPS Ra (**B**) or 1 ng/ml S-form LPS (**C**) at the indicated peptide concentrations. The mixtures were used to activate human MNCs. As a marker of LPS-induced cell activation, the production of the cytokine TNFα was determined by ELISA.

cations from the backbone of an LPS Re monolayer at the air/water interface was investigated (Figure 3). Here, LF11 has a slightly higher capacity than lauryl-LF11 to displace LPS-bound calcium. Both peptides displaced all cations at a peptide/LPS ratio of approx. 3. Therefore higher antimicrobial and endotoxin-neutralizing activities of the acylated form of the peptide are not due to the replacement of cations stabilizing the LPS layer.

Compensation of the accessible surface charges of LPS aggregates (zeta potential) by the peptides

As a measure for the accessible surface charges in LPS aggregates, the zeta potential was determined for LPS Re and Ra by measuring their electrophoretic mobility at different peptide concentrations (Figure 4). For LPS Re with a short sugar chain, LF11 compensates the surface charges of LPS at a peptide/LPS molar ratio of 2. For LPS Ra, the charge is compensated to −5 mV at a peptide/LPS molar ratio of 4. Complete compensation, extrapolated from the curve, may be reached at a peptide/LPS molar ratio of approx. 5–6. In contrast, lauryl-LF11 overcompensates the surface charges of LPS Re and Ra, indicating that, besides electrostatic interaction, a further process, hydrophobic interaction, takes place. The charge compensation (zero zeta potential) is reached for LPS Re at a molar peptide/LPS ratio below 1, whereas this ratio is approx. 2.5 for LPS Ra.

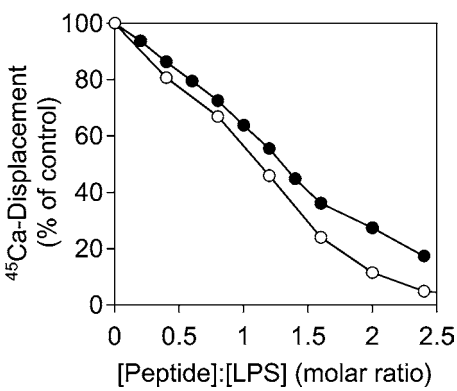

Figure 3 Displacement of ^{45}Ca from LPS Re monolayers by cationic peptides

LF11 (○) and lauryl-LF11 (●) were injected in the subphase under an LPS Re monolayer saturated with ^{45}Ca. Peptide binding resulted in the displacement of calcium accompanied by a decrease in radioactivity.

Peptide–LPS-binding enthalpies

For the elucidation of the stoichiometry of peptide–LPS binding, ITC (isothermal titration calorimetry) performed at 37 °C was

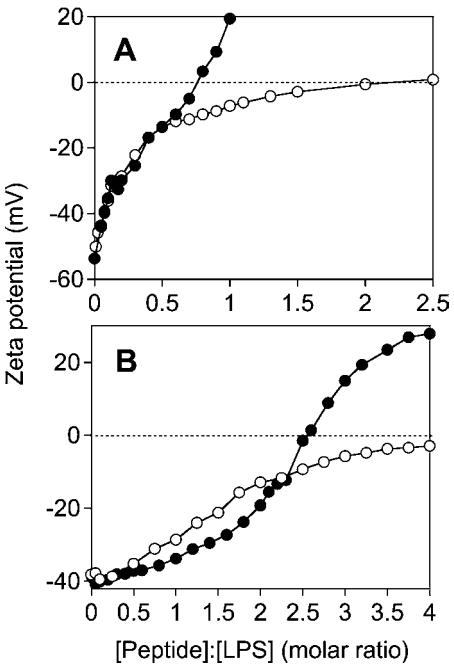

Figure 4 Dependence of zeta potential of LPS preparations (A, LPS Re; B, LPS Ra) on different peptide/LPS molar ratios

LF11 (○) and lauryl-LF11 (●) were titrated against LPS suspensions and the zeta potential was determined from the electrophoretic mobility analysed by laser-Doppler anemometry. Note the charge overcompensation for lauryl-LF11.

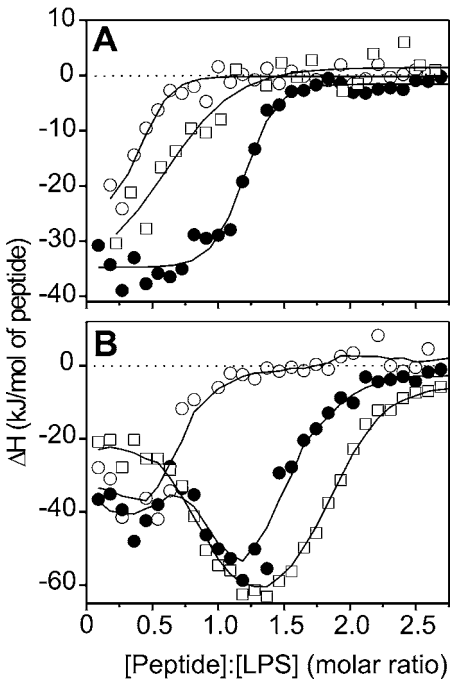

Figure 5 Enthalpy change of the peptide-LPS (○, LPS Re; ●, LPS Ra; □, S-form LPS) binding reaction as a function of various peptide/LPS molar ratios from calorimetric titration curves

(**A**) LF11; (**B**) lauryl-LF11. Positive and negative ΔH values indicate endothermic and exothermic reactions respectively.

applied. The results of LF11 binding to three LPS chemotypes are shown in Figure 5(A), those of lauryl-LF11 binding to LPS are shown in Figure 5(B). Clearly, for both peptides and all LPS chemotypes, only exothermic (negative enthalpy change) processes are observed, indicating dominant electrostatic interactions. Furthermore, differences in binding saturation are observed which may be correlated with the length of the LPS sugar chains. Thus, for LF11 binding to LPS, saturation is observed at an LF11/LPS Re molar ratio of approx. 0.8, and for the two LPS with longer sugar chains, the ratio is between 1.3 and 1.7. Similarly, the binding of lauryl-LF11 to the LPS is saturated at a lauryl-LF11/LPS molar ratio of approx. 1.25 for LPS Re, and above 2.2–2.5 for LPS Ra and S-form LPS. Moreover, the binding of S-form LPS is biphasic, starting with a plateau at approx. -20 to -40 kJ/mol at lower peptide concentrations, and a maximum at approx. -50 to -60 kJ/mol at a lauryl-LF11/LPS molar ratio of between 1.0 and 1.5.

Influence of the peptides on the phase behaviour of LPS acyl chains

The gel-to-liquid-crystalline phase-transition of the acyl chains of LPS in the presence of different amounts of peptides was monitored by plotting the peak positions of the symmetric stretching vibration $\nu_s(CH_2)$ against temperature (Figure 6). LF11 causes only a very slight change in the transition curve of LPS Re, for which the phase-transition temperature (T_c) lies at approx. 31 °C. In contrast with LPS Ra, LF11 induces a clear increase in the wavenumbers, corresponding to the fluidization of the acyl chains. The action of lauryl-LF11 is similar for both LPS, a fluidization occurs in particular in the gel phase, which is strong for LPS Re and weaker for LPS Ra.

The thermodynamic parameters of pure LPS Re as obtained from DSC are: $T_c = 31.0$ °C, half-width $T_{1/2} = 7$ °C and phase-transition enthalpy $\Delta H_c = 39.4$ kJ/mol. The presence of LF11 induces a 1–2 °C increase in T_c, whereas the phase-transition enthalpy remains unchanged ($\Delta H_c \sim 39 \pm 2$ kJ/mol). A slight decrease in T_c of 1–2 °C and a slight decrease in ΔH_c of ~10–15% are observed for the lauryl-LF11/LPS Re mixtures (results not shown). The thermodynamic parameters of the pure LPS Ra are determined as: $T_c = 36.2$ °C, $T_{1/2} = 11$ °C and $\Delta H_c = 19$ kJ/mol. The presence of LF11 induces a shift in the maximum of the heat-capacity curve to lower temperature (Figure 7A). At an equimolar LF11/LPS Ra ratio, T_c is lowered to 33.0 °C, indicating a destabilization of the gel phase. Additionally, a large decrease in the phase-transition enthalpy is observed. Compared with ΔH_c of the pure endotoxin, ΔH_c of an equimolar LF11/LPS Ra mixture is decreased by more than 60%. This can be interpreted as a strong decrease in the van der Waals interactions between the hydrophobic acyl chains of the LPS Ra in the presence of an equimolar peptide/LPS mixture.

The synthetic peptide lauryl-LF11 also induces a considerable decrease in the phase-transition enthalpy of the gel-to-liquid-crystalline phase-transition of LPS Ra. However, only a marginal T_c shift is observed for the equimolar system from 36.1 °C (pure LPS Ra) to 35.7 °C (Figure 7B). This is in accordance with the FTIR data.

Influence of the peptides on the LPS-aggregate structure

Synchrotron radiation X-ray diffraction was used to investigate the aggregate structure of lipid A (as the 'endotoxic principle' of LPS) in the absence and presence of the peptides (Figure 8). Pure lipid A adopts a mixed cubic/unilamellar structure in accordance with earlier results [20], which can be deduced from the broad scattering intensity maximum between 0.1 and 0.4 nm^{-1}, and some weak reflections superimposed (Figure 8A). In the presence of the peptides, the diffraction patterns change with small, but

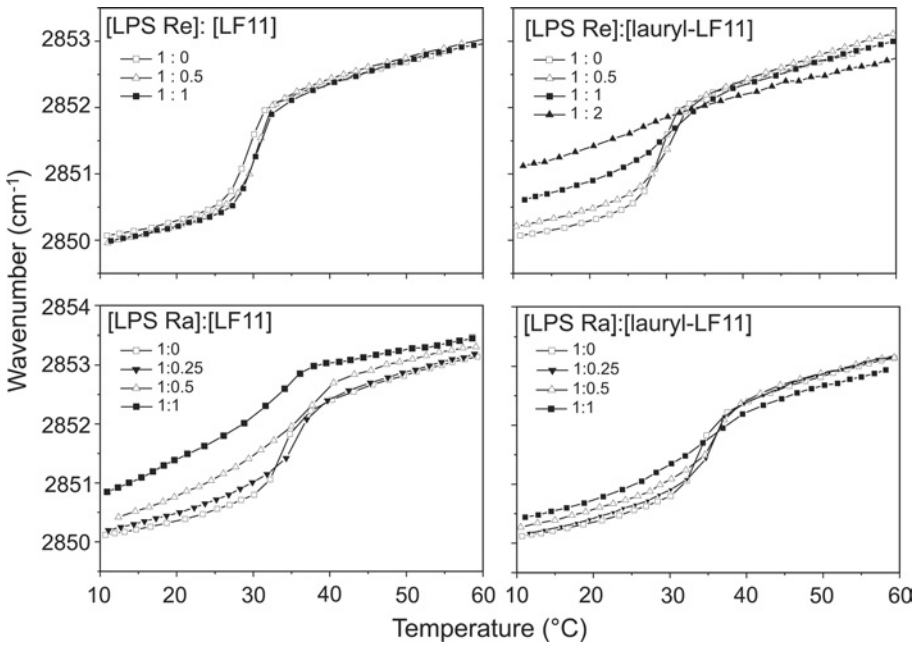

Figure 6 Phase-transition behaviour of LPS Re and LPS Ra in the presence of LF11 and lauryl-LF11, monitored over the peak position of the symmetric stretching vibration of the methylene groups of LPS acyl chains at different LPS/peptide molar ratios

In the gel (β) phase of the acyl chains, the peak lies at approx. 2850 cm^{-1}; in the liquid-crystalline (α) phase, the peak lies at approx. 2852.5 cm^{-1}.

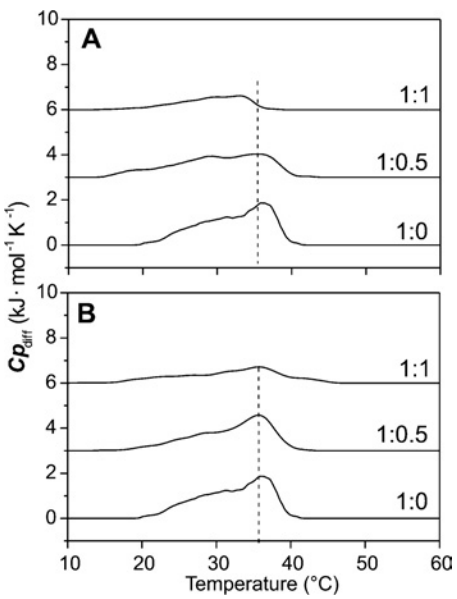

Figure 7 Heat-capacity curves, Cp_{diff}, against temperature of various LPS Ra/peptide mixtures from DSC scans

(**A**) LF11; (**B**) lauryl-LF11.

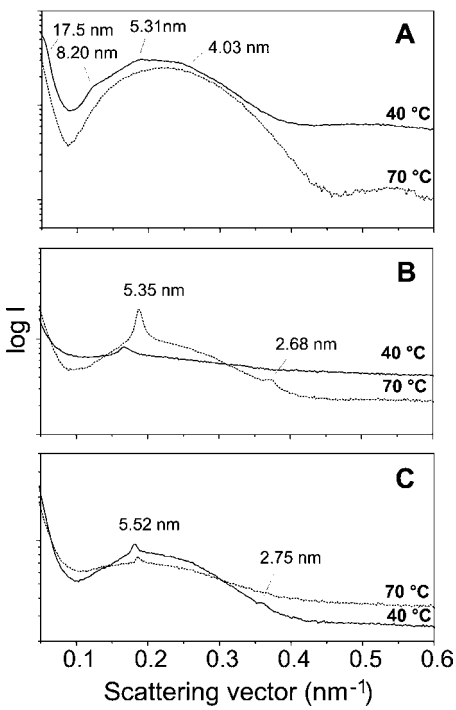

Figure 8 Small-angle X-ray diffraction patterns of lipid A from *S. enterica* (serovar Minnesota) R595 LPS Re at 90% water content and 40 °C without peptide (A) and in the presence of LF11 (B) and lauryl-LF11 (C), at a peptide/LPS molar ratio of 10:1

sharp, equidistant reflections (e.g. 5.35 nm and 2.68 nm for lipid A/LF11; Figure 8B) corresponding to multilamellar stacks.

DISCUSSION

LF is a multifunctional protein with antibacterial, antiviral, antitumour and anti-inflammatory properties [1], which are related to a 25-amino-acid-residue N-terminal fragment called lactoferricin. Bovine lactoferricin derivatives have been described which were able to cross the cell walls and cytoplasmic membranes of both Gram-negative and Gram-positive bacteria [21]. Lactoferricin derivatives corresponding to the amphipathic α-helical region of human LF disrupt outer membranes of Gram-negative bacteria [4,22] and neutralize endotoxin *in vitro* and *in vivo*

(LF-33; [7]). The test of various lactoferricin derivatives from milk LF showed that many of these compounds have high antimicrobial activity [3].

We have designed a synthetic derivative corresponding to amino acid residues 21–31 of human lactoferricin as a starting material, in which the isoleucine was substituted for the methionine residue ($Met^{27} \rightarrow Ile$) to increase peptide stability. Furthermore, the peptide lauryl-LF11 was designed, since the addition of a 12-carbon-units acyl chain has been shown to enhance antibacterial and LPS-binding activities of the peptide [8]. The comprehensive physicochemical and biological analysis of the interaction of the peptides with LPS, as previously performed for, e.g., LF and the antimicrobial peptide NK-2 [23,24], showed that the introduction of the lauryl chain enhanced the antibacterial activity against bacteria with LPS Re, but not against those with LPS Ra and S-form (Figure 1), which have a much longer sugar chain and, with that, reduced hydrophobicity compared with LPS Re. Notably, the activity of LF11 against *S. enterica* reported in the present paper is much more pronounced than the anti-*Escherichia coli* activity of the LF(21-31) peptide described by Chapple et al. [22], which has an almost identical primary structure with LF11 with the exception of the methionine/isoleucine substitution mentioned above. These differences in activity are most likely based upon the C-terminal amidation of LF11, which enhances the effective positive net charge of the peptide and thus strengthens the interaction with negatively charged bacterial surface.

In the TNFα-induction assay, reflecting neutralization of biological activity of LPS (Figure 2), however, lauryl-LF11 was more active than LF11 for all LPS chemotypes. For an interpretation, it has to be taken into account that, in bacteria, the sugar part of LPS is directed towards the outside and represents a barrier for the peptides solely due to steric reasons [24], which is low for the LPS with short-sugar chains (LPS Re). In the cytokine assay, peptides interact with LPS aggregates, and the accessibility of the binding epitopes in the LPS backbone might be completely different. In this context, it should be noted that the aggregation state of the peptides may also influence its interaction with LPS and thus its biological activities. For a lauryl-peptide, very similar to LF11, we observed a CMC (critical micelle concentration) of 0.4 mM, whereas for the same peptide without the lauryl moiety, the CMC value is significantly higher than 10 mM (results not shown). Thus aggregation effects of lauryl-LF11 have to be considered for those assays where the peptide concentration exceeds the CMC, i.e. the FTIR and SAXS (small-angle X-ray scattering) measurements.

Peptide binding to LPS can be interpreted, at least initially, to be electrostatic and to result from the attraction between the positive charges (lysine and arginine side chains) of the peptides and the negative charges (phosphates and carboxylates) of LPS. This can be deduced from the data of the Ca^{2+} replacement of LPS Re (Figure 3), and also from the reduction of the zeta potential, leading to binding compensation of LPS Re as well as LPS Ra (Figure 4). Beyond charge compensation, however, for lauryl-LF11, a further increase of the zeta potential with strongly positive values is observed, i.e. for this compound, a hydrophobic interaction of the acyl chain residue with the lipid A moiety also takes place. This can be deduced in a similar way from the ITC curves, leading to a biphasic behaviour for LPS Ra and S-form (Figure 5A), and much higher values for the binding stoichiometry of lauryl-LF11 compared with those of LF11 (Figures 5A and 5B).

The differences in hydrophobicity of the two peptides also becomes evident from the data of the phase-transition behaviour (Figure 6): LF11 induces only a small effect on LPS Re, and, on the other hand, lauryl-LF11 has a small effect on LPS Ra, i.e. the more hydrophilic peptide interacts less favourably with the more hydrophobic LPS and vice versa. The addition of LF11 to LPS Ra leads to the fluidization of the acyl chains in the whole temperature range, whereas addition of lauryl-LF11 to LPS Re increases fluidization of the acyl chains in the gel phase, and slight rigidification in the liquid crystalline phase. The latter is also true for lauryl-LF11 on LPS Ra, and is indicative of the cholesterol-like effect [25,26] of this lipopeptide.

Comparison of the peptide neutralization of LPS with those of integral human LF show a considerably higher activity of the latter on a molar scale, leading to inhibition of the TNFα-production already at an equimolar ratio of LPS Re and LF [23]. Regarding the high MM of LF (80000 Da), however, the activity becomes similar at least for LPS Re and lauryl-LF11 if calculated on a mass scale. An important consideration is the presence of two LPS-binding sites on LF, which contributes to the co-operativity of LPS binding [27]. A comparison of the interaction mechanism of the protein/peptides with LPS shows that, at binding saturation of LF, a remaining zeta potential of -10 mV is observed, in contrast with the complete neutralization of LPS Re found in the present study. Furthermore, also in contrast with the results obtained in the present study for the peptides, a clear rigidification of the acyl chains of LPS, connected with an increase in the phase transition temperature T_c, due to LF binding, takes place. These differences may be indicative of large steric differences, allowing the small peptides to interact more easily with the LPS backbone than with the bulky protein.

Both peptides and LF behave similarly as far as the aggregate structure is concerned, and the 'endotoxic principle' lipid A adopts a multilamellar structure in their presence (Figure 8). It was found, not only for LF and the LF-derived peptides described in the present study, but also for other proteins and peptides, that the inactivation of LPS is accompanied by a change of the aggregate structure of lipid A or LPS into a multilamellar form [23,24,28–31]. From the analysis of lipid A compounds with different chemical structures, it was found that a non-lamellar or mixed unilamellar/non-lamellar structure represents the active, and a multilamellar structure the inactive form of endotoxins [32,33]. Thus highly active hexa-acyl lipid A of enterobacterial origin, such as that from *E. coli*, has a cubic or a mixed unilamellar/cubic structure, whereas agonistically inactive penta- and tetra-acyl forms from *E. coli* mutants or of synthetic origin adopt multilamellar structures [32]. The conversion observed here and for LF is similar to that observed for binding of lysozyme [29] and HDL (high-density lipoprotein) [28] to lipid A, but different from binding of Hb [11] and rHSA (recombinant human serum albumin) [34], for which the lipid A aggregate structure is changed into another non-lamellar, probably also a cubic, structure with a different symmetry [34]. These observations suggest that an apparent prerequisite for neutralization of LPS by binding proteins or peptides is the change of the aggregate structure of its lipid A moiety into a multilamellar one. Multilamellar stacks of LPS are facilitated by compensation of electrostatic repulsion energy between anionic polar heads of LPS due to the peptide charge compensation. For an interpretation of the fact that the multilamellar structure of a given lipid A, whether alone or after binding to proteins, is directly correlated with endotoxic inactivity, the following points should be considered. The endotoxin-induced cell activation is initiated by the interaction of serum-proteins such as LBP (LPS-binding protein) and membrane-bound proteins such as CD14 with LPS [35–37], followed by transport to transmembrane signalling molecules, such as the TLR4 (Toll-like receptor 4)–MD-2 complex or the MaxiK ion channel [38,39] and subsequent signalling to the cell interior. Within these complex interaction mechanisms, the following processes seem to be of relevance. (i) LPS aggregates are very stable. The binding energy

of one LPS molecule with a hexa-acyl lipid A portion within an aggregate has been determined to be lower than -400 meV [40]. Thus, to remove LPS monomers, the binding energy of LPS-recognition proteins such as LBP, CD14 or MD-2 to LPS must exceed this amount. Although the dependence of binding energy on the type of aggregate structure is unknown, it is plausible that a monomer within multilamellar stacks is more stably bound than, for example, within an unilamellar structure. (ii) The accessibility of the recognition structures (epitopes) within the LPS molecules. The eukaryotic LBPs recognize a certain structural pattern within the LPS molecule, which is probably a pattern in the lipid A backbone. It is obvious that the type of aggregate structure influences this recognition process. Thus, in multilamellar structures, most of the lipid A backbones are hidden and not accessible to the binding proteins, in contrast with the situation in unilamellar or cubic structures.

In summary, we significantly enhanced the endotoxin-neutralizing capacity of the LF LPS-binding domain by N-terminal linkage with a 12-carbon-units alkyl chain. We undertook a comprehensive biophysical characterization of the interaction of these synthetic peptides with LPS with variations in the sugar length. The neutralization of the LPS surface charges is a prerequisite, but not sufficient, for an effective neutralization of the cell-activation activity of LPS by cationic peptides. A significant increase in inhibitory activity was observed if a hydrophobic interaction occurs, which results in a significant overcompensation of the negative surface charge of LPS aggregates. This was observed in the present study for lauryl-LF11 and has also been described recently for synthetic peptides derived from NK-lysin and LALF (*Limulus* anti-LPS factor) [24,31]. We suggest that the peptide–LPS affinity must be able to compete with the LPS–LBP interaction [24]. This is likely to be achieved by a combination of electrostatic interactions of the positively charged amino acid side chains of the peptides with the LPS backbone phosphate groups and a penetration of the hydrophobic core of the LPS aggregate.

We thank G. von Busse, K. Stephan and B. Fölting for assistance with the FTIR, TNFα and DSC measurements respectively. The study has been carried out with financial support from the Commission of the European Communities, specific RTD programme 'Quality of Life and Management of Living Resources', QLCK2-CT-2002-01001, "Antimicrobial endotoxin neutralizing peptides to combat infectious diseases".

REFERENCES

1 Vogel, H. J., Schibli, D. J., Jing, W., Lohmeier-Vogel, E. M., Epand, R. F. and Epand, R. M. (2002) Towards a structure–function analysis of bovine lactoferricin and related tryptophan- and arginine-containing peptides. Biochem. Cell Biol. **80**, 49–63
2 Baynes, R. D. and Bezwoda, W. R. (1994) Lactoferrin and the inflammatory response. In Lactoferrin: Structure and Function (Hutchens, T. W., Lönnerdal, B. and Rumball, S., eds.), Plenum Press, New York
3 Wakabayashi, H., Takase, M. and Tomita, M. (2003) Lactoferricin derived from milk protein lactoferrin. Curr. Pharm. Des. **9**, 1277–1287
4 Chapple, D. S., Mason, D. J., Joannou, C. L., Odell, E. W., Gant, V. and Evans, R. W. (1998) Structure–function relationship of antibacterial synthetic peptides homologous to a helical surface region on human lactoferrin against *Escherichia coli* serotype O111. Infect. Immun. **66**, 2434–2440
5 Zähringer, U., Lindner, B. and Rietschel, E. T. (1994) Molecular structure of lipid A, the endotoxic center of bacterial lipopolysaccharides. Adv. Carbohydr. Chem. Biochem. **50**, 211–276
6 Rietschel, E. T., Brade, H., Holst, O., Brade, L., Müller-Loennies, S., Mamat, U., Zähringer, U., Beckmann, F., Seydel, U., Brandenburg, K. et al. (1996) Bacterial endotoxin: chemical constitution, biological recognition, host response, and immunological detoxification. Curr. Top. Microbiol. Immunol. **216**, 39–81
7 Zhang, G., Mann, D. and Tsai, C. (1999) Neutralization of endotoxin *in vitro* and *in vivo* by a human lactoferrin-derived peptide. Infect. Immun. **67**, 1353–1358
8 Majerle, A., Kidric, J. and Jerala, R. (2003) Enhancement of antibacterial and lipopolysaccharide binding activities of a human lactoferrin peptide fragment by the addition of acyl chain. J. Antimicrob. Chemother. **51**, 1159–1165
9 Galanos, C., Lüderitz, O. and Westphal, O. (1969) A new method for the extraction of R lipopolysaccharides. Eur. J. Biochem. **9**, 245–249
10 Westphal, O., Lüderitz, O. and Bister, F. (1952) Über die Extraktion von Bakterien mit Phenol/Wasser. Z. Naturforsch. **7**, 148–155
11 Brandenburg, K., Garidel, P., Andrä, J., Jürgens, G., Müller, M., Blume, A., Koch, M. H. J. and Levin, J. (2003) Cross-linked hemoglobin converts endotoxically inactive pentaacyl endotoxins into a physiologically active conformation. J. Biol. Chem. **278**, 47660–47669
12 Ohtani, Y., Irie, T., Uekama, K., Fukunaga, K. and Pitha, J. (1989) Differential effects of α-, β- and γ-cyclodextrins on human erythrocytes. Eur. J. Biochem. **186**, 17–22
13 Mosmann, T. (1983) Rapid colorimetric assay for cellular growth and survival: application to proliferation and cytotoxicity assays. J. Immunol. Methods **65**, 55–63
14 Hudson, L. and Hay, F. C. (1976) Practical Immunology, Blackwell Scientific Publishers, Oxford
15 Blume, A. and Garidel, P. (1999) Lipid model membranes and biomembranes. In The Handbook of Thermal Analysis and Calorimetry (Kemp, R. B., ed.), pp. 109–173, Elsevier, Amsterdam
16 Gutsmann, T., Hagge, S. O., Larrick, J. W., Seydel, U. and Wiese, A. (2001) Interaction of CAP18-derived peptides with membranes made from endotoxins or phospholipids. Biophys. J. **80**, 2935–2945
17 Koch, M. H. J. and Bordas, J. (1983) X-ray diffraction and scattering on disordered systems using synchrotron radiation. Nucl. Instrum. Methods **208**, 461–469
18 Gabriel, A. (1977) Position-sensitive X-ray detector. Rev. Sci. Instrum. **48**, 1303–1305
19 Boulin, C., Kempf, R., Koch, M. H. J. and McLaughlin, S. M. (1986) Data appraisal, evaluation and display for synchrotron radiation experiments: hardware and software. Nucl. Instrum. Methods **249**, 399–407
20 Brandenburg, K., Richter, W., Koch, M. H. J., Meyer, H. W. and Seydel, U. (1998) Characterization of the nonlamellar cubic and H_{II} structures of lipid A from *Salmonella enterica* serovar Minnesota by X-ray diffraction and freeze-fracture electron microscopy. Chem. Phys. Lipids **91**, 53–69
21 Haukland, H. H., Ulvatne, H., Sandvik, K. and Vorland, L. H. (2001) The antimicrobial peptides lactoferricin B and magainin 2 cross over the bacterial cytoplasmic membrane and reside in the cytoplasm. FEBS Lett. **508**, 389–393
22 Chapple, D. S., Hussain, R., Joannou, C. L., Hancock, R. E., Odell, E., Evans, R. W. and Siligardi, G. (2004) Structure and association of human lactoferrin peptides with *Escherichia coli* lipopolysaccharide. Antimicrob. Agents Chemother. **48**, 2190–2198
23 Brandenburg, K., Jürgens, G., Müller, M., Fukuoka, S. and Koch, M. H. J. (2001) Biophysical characterization of lipopolysaccharide and lipid A inactivation by lactoferrin. Biol. Chem. **382**, 15–25
24 Andrä, J., Koch, M. H. J., Bartels, R. and Brandenburg, K. (2004) Biophysical characterization of the endotoxin inactivation by NK-2, an antimicrobial peptide derived from mammalian NK-lysin. Antimicrob. Agents Chemother. **48**, 1593–1599
25 Corvera, E., Mouritsen, O. G. and Singer, M. A. (1992) The permeability and the effect of acyl-chain length for phospholipid bilayers containing cholesterol: theory and experiment. Biochim. Biophys. Acta **1107**, 261–270
26 Urbina, J. A., Pekerar, S., Le, H. B., Patterson, J., Montez, B. and Oldfield, E. (1995) Molecular order and dynamics of phosphatidylcholine bilayer membranes in the presence of cholesterol, ergosterol and lanosterol: a comparative study using ^{2}H-, ^{13}C- and ^{31}P-NMR spectroscopy. Biochem. Biophys. Acta **1238**, 163–176
27 Elass-Rochard, E., Roseanu, A., Legrand, D., Trif, M., Salmon, V., Motas, C., Montreuil, J. and Spik, G. (1995) Lactoferrin–lipopolysaccharide interaction: involvement of the 28–34 loop region of human lactoferrin in the high-affinity binding to *Escherichia coli* 055B5 lipopolysaccharide. Biochem. J. **312**, 839–845
28 Brandenburg, K., Jürgens, G., Andrä, J., Lindner, B., Koch, M. H. J., Blume, A. and Garidel, P. (2002) Biophysical characterization of the interaction of high-density lipoprotein (HDL) with endotoxins. Eur. J. Biochem. **269**, 5972–5981
29 Brandenburg, K., Koch, M. H. J. and Seydel, U. (1998) Biophysical characterization of lysozyme binding to LPS Re and lipid A. Eur. J. Biochem. **258**, 686–695
30 Andrä, J., Garidel, P., Majerle, A., Jerala, R., Ridge, R., Paus, E., Novitsky, T., Koch, M. H. J. and Brandenburg, K. (2004) Biophysical characterization of the interaction of *Limulus polyphemus* endotoxin neutralizing protein (ENP) with lipopolysaccharide. Eur. J. Biochem. **271**, 2037–2046
31 Andrä, J., Lamata, M., Martinez de Tejada, G., Bartels, R., Koch, M. H. J. and Brandenburg, K. (2004) Cyclic antimicrobial peptides based on *Limulus* anti-LPS factor for neutralization of lipopolysaccharide. Biochem. Pharmacol. **68**, 1297–1307
32 Schromm, A. B., Brandenburg, K., Loppnow, H., Moran, A. P., Koch, M. H. J., Rietschel, E. T. and Seydel, U. (2000) Biological activities of lipopolysaccharides are determined by the shape of their lipid A portion. Eur. J. Biochem. **267**, 2008–2013
33 Seydel, U., Oikawa, M., Fukase, K., Kusumoto, S. and Brandenburg, K. (2000) Intrinsic conformation of lipid A is responsible for agonistic and antagonistic activity. Eur. J. Biochem. **267**, 3032–3039

34 Jürgens, G., Müller, M., Garidel, P., Koch, M. H. J., Nakakubo, H., Blume, A. and Brandenburg, K. (2002) Investigation into the interaction of recombinant human serum albumin with Re-lipopolysaccharide and lipid A. J. Endotoxin Res. **8**, 115–126
35 Delude, R. L., Savedra, Jr, R., Zhao, H., Thieringer, R., Yamamoto, S., Fenton, M. J. and Golenbock, D. T. (1995) CD14 enhances cellular responses to endotoxin without imparting ligand-specific recognition. Proc. Natl. Acad. Sci. U.S.A. **92**, 9288–9292
36 Wright, S. D., Ramos, R. A., Tobias, P. S., Ulevitch, R. J. and Mathison, J. C. (1990) CD14, a receptor for complexes of lipopolysaccharide (LPS) and LPS binding protein. Science **249**, 1431–1433
37 Chow, J. C., Young, D. W., Golenbock, D. T., Christ, W. J. and Gusovsky, F. (1999) Toll-like receptor-4 mediates lipopolysaccharide-induced signal transduction. J. Biol. Chem. **274**, 10689–10692
38 Beutler, B. (2000) Tlr4: central component of the sole mammalian LPS sensor. Curr. Opin. Immunol. **12**, 20–26
39 Blunck, R., Scheel, O., Müller, M., Brandenburg, K., Seitzer, U. and Seydel, U. (2001) New insights into endotoxin-induced activation of macrophages: involvement of a K^+ channel in transmembrane signaling. J. Immunol. **166**, 1009–1015
40 Buschner, S. (1999) Bestimmung der Kritischen Aggregatkonzentrationen von Lipiden: Implikationen für die Biologische Wirksamkeit von Endotoxinen, Ph.D. Thesis, Universität Kiel, Kiel, Germany

Received 27 July 2004/27 August 2004; accepted 2 September 2004
Published as BJ Immediate Publication 2 September 2004, DOI 10.1042/BJ20041270